Asian Journal of Civil Engineering (2023) 24:2645–2657
https://doi.org/10.1007/s42107-023-00669-3

RESEARCH

Dynamic response of high-rise buildings with shear walls due to seismic forces

Kashyap Shukla[1] · **K. Nallasivam**[1]

Received: 14 April 2023 / Accepted: 17 April 2023 / Published online: 23 April 2023
© The Author(s), under exclusive licence to Springer Nature Switzerland AG 2023

Abstract

Lateral loads such as earthquake and wind loads play a governing role in the design of high-rise buildings. Consequently, the vital work in the lives of structural engineers is to minimise damage to the structure and its structural components during an earthquake by proper design. A shear wall is one of the vertical elements that fulfil the above function by providing enough lateral rigidity if it is located and arranged effectively. As a result, the purpose of the study is to determine the response of various high-rise buildings with different shear wall arrangements when subjected to seismic loads. A total of nine G + 30-storey models have been made using finite element-based ETABS software. All the models have shear walls distributed in such a way that the floor plan length of the walls is the same in all buildings, so the results are influenced solely by the arrangement and location of the walls. Seismic loads were applied using the response spectrum method, which complied with Indian codal provisions. The results of storey displacements, the storey drifts and storey shear were extracted. The shear walls arranged in the form of a core at the centre of the building have been the most effective. It shows a 1.8 times greater decrement in top-storey displacement compared to the model without shear walls. The building with an irregular arrangement of shear walls at the corner is the least effective in resisting earthquakes.

Keywords High-rise buildings · Shear wall · Response spectrum analysis · ETABS models

Introduction

Due to increasing urbanisation and population growth, there is a high demand for the construction of high-rise buildings all over the world, and earthquakes have the potential to cause the most damage to those high-rise structures. In such cases, the provision of lateral stiffness becomes critical for building. Columns and shear walls are the two primary types of vertical load-resisting elements. The latter provides more stiffness. Shear walls are vertical plate-like reinforced concrete walls that extend from the foundation level to the full height of the building to form a vertical cantilever (Murty, 2005). Due to lateral loads, it is subjected to in-plane shear forces. Shear walls are suitable for use in buildings up to 35 storeys due to their higher in-plane stiffness (Smith & Coull, 1991). Wang et al. (2001) investigated the impact of shear wall height on the earthquake response of frame–shear wall structures. They noticed the marginal influence of shear wall height on the effective stiffness of some buildings. Fan et al. (2009) created a model of the Taipei Financial Centre, which has 101 storeys and a height of 508 m, and analysed it by the time history method with the use of scaled accelerograms to quantify earthquake occurrences with a return period of 50-year, 100-year and 950-year, respectively.

Kaveh et al. (2010) attempted the ant colony optimization (ACO) method and a genetic algorithm (GA) to perform the seismic design of steel frames with four performance levels. When compared to other evolutionary approaches, this discrete metaheuristic algorithm significantly improves consistency and computational efficiency. To determine the structural response at various seismic performance levels, a non-linear analysis is used, which employs a simple computer-based method for push-over analysis that accounts for first-order elastic and second-order geometric stiffness features. Kaveh and Talatahari (2010) provide a revised iterative ant colony optimization (IACO) method for designing planar steel frames. The algorithm is divided into two phases: global search and local search. The proposed method has been examined on many planar steel frames and

✉ K. Nallasivam
nallasivam_iit_nit@yahoo.co.in

[1] National Institute of Technology Hamirpur, Hamirpur, Himachal Pradesh, India

compared to those of the regular ant colony optimization, the genetic algorithm, and the harmony search algorithm in this study. Abd-el-Rahim and Farghaly (2010) investigated the effect of an edge shear wall in a slender building supported by a raft foundation. For this study, various models were created, each with a different subgrade modulus, and then analysed using the time history method in SAP2000 software. Bhatt and Bento (2012) performed a seismic assessment of two existing five- and eight-storey buildings with the asymmetric plan in Turkey by comparing the results of non-linear dynamic and non-linear static analyses, which consists of inter-storey drifts, normalised top displacements, lateral displacement profiles, chord rotations, base shear and top displacement ratios. Kaveh and Zakian (2013) optimised the design of steel frames subjected to seismic force. The cross-sectional areas of the member variables are discrete and are chosen from a list of existing cross-sections. For optimisation, the charged system search and enhanced harmony search algorithms are used. A time history analysis with relative lateral displacement constraints is performed in the first phase for the optimal design of steel frames, and a simultaneous dynamic-static analysis with relative displacement and stress constraints is performed in the second phase using two metaheuristic algorithms.

Kaveh and Talatahari (2012) suggested a discrete version of CSS for optimal frame structure design. The suggested technique allows charged particles to choose discrete values from a list of allowable cross-sections, and if any of them chooses another value for a design variable, the CSS changes its value to the nearest discrete cross-section. CSS is compared to various well-known metaheuristic algorithms to show its specific qualities. Three frame architectures are investigated to validate the implied algorithm's efficiency. Kaveh et al., (2014a, 2014b) discovered two simplifying strategies to be very effective in dealing with the problem: first, simplified non-linear modelling investigating the lowest level of structural modelling sophistication, and second, wavelet analysis of earthquake records reducing the number of acceleration points involved in time history loading. They try to establish an efficient framework using both methodologies to address the performance-based multi-objective optimal design issue of steel moment-frame structures whilst taking into account the initial cost and the seismic damage cost. Kaveh et al., (2014a, 2014b) formed a damage-based seismic design technique for steel frame buildings as an optimisation problem, to minimise the initial construction cost. The design procedure's performance limitation is to produce a “repairable” damage condition for earthquake demands that are less severe than the design ground movements. The Park-Ang damage index is chosen as the seismic damage metric for structural damage quantification. To find the best solutions, the charged system search (CSS) method is used as the optimisation technique. Two simplifying strategies are used to improve the time efficiency of the solution algorithm: first, SDOF idealisation of multi-storey building structures capable of estimating the actual seismic response in a very short time; and second, fitness approximation, which reduces the number of fitness function evaluations.

Kaveh and Zakian (2014) focussed on an optimisation challenge for the seismic design of reinforced concrete (RC) dual systems and RC frames. The first databases are built using ACI seismic design criteria for beams, columns and shear walls. Formulations for optimal seismic design of dual systems (shear wall-frame) with certain alterations to these formulae, optimum seismic design of RC moment-resistant frames are done. Tuppad and Fernandes (2015) investigated the optimal positioning of a shear wall in a G + 10-storey building under seismic load. Six models were created using ETABS, one without a shear wall and the other five with a shear wall at various locations. Seismic loads were applied using the equivalent static method. The genetic algorithm was also used for optimisation, and it was determined that the shear wall at the centre produces the best results. To perform a seismic analysis on a structure, the actual time history at the specific location must be known, which is not always possible. Furthermore, seismic analysis based on maximum ground acceleration cannot provide accurate results because the response of a structure is also a parameter of the frequency content of ground motion and dynamic properties of the structure. To overcome the aforementioned limitations, the response spectrum method is a useful tool in structural seismic analysis. The method calculates only the maximum values of displacements and member forces in each mode of vibration by taking the mean of several earthquake motions to construct smooth design spectra. It is useful for structures where modes affect the structure’s response. This research focuses on multi-storey rectangular buildings with varying shear wall arrangements, which were modelled using the ETABS software. To determine earthquake loads, the response spectrum method specified in IS, 1893, Part-1 (2016) was used.

Titiksh and Bhatt (2017) created four different ETABS buildings to demonstrate the effectiveness of shear wall positioning against lateral loads. For resolving the difficulty, Kaveh and Bolandgerami (2017) used the cascade optimisation approach, which enables a single optimisation problem to be handled in several sequential independent optimisation phases. To test the efficacy of this strategy, the optimisation algorithm used in all phases of the cascade process is improved colliding bodies optimisation, which is a strong metaheuristic. Udaya et al.(2018) used the response spectrum and time history method to perform dynamic analysis on an R.C.C. structure with 3 basements, a ground floor and 14 upper floors in zone IV. The results of maximum storey displacement, maximum storey drift and spectrum

displacement were compared for buildings with only flat slabs and buildings with flat slabs and shear walls. Akhil-Ahamad and Pratap (2020) used response spectrum analysis to investigate the effects of shear wall placement in a 20-storey residential building. Three models were created using ETABS: one with no shear wall, one with shear walls situated at two adjacent corners of the structure and one with shear walls at each corner. Buildings with shear walls on all four corners outperform others because their displacement, drift and base shear are lower. Agha and Umamaheswari (2020) presented research work on irregular RCC buildings with only shear walls, as well as dual-framed shear wall systems subjected to seismic loads calculated using both the equivalent static method and the response spectrum method. Ghayoumian and Emami(2020) developed three models with the same shear wall arrangement but a different number of storeys: four, eight, and twelve. They assessed the seismic response of modern buildings with torsional irregularities in a 3D perspective using the distribution of inter-storey drift, ductility and damage indices. Zakian and Kaveh (2023) reviewed seismic design optimisation of structures, concentrating on common solution approaches, optimisation issue types and optimisation aims. The primary goal of the research is to find a shear wall arrangement that will effectively resist load whilst exhibiting minimal displacement. The storey displacement, drift and shear due to earthquakes are compared between buildings with different shear wall arrangements.

Methods

Modelling of the multi-storey building

The first step in the study is to model high-rise buildings. The ETABS finite element software was used to model nine G + 30-storey buildings. The first model is a rectangular building with no shear walls, and the remaining eight models are various shear wall layouts in rectangular buildings. All of these models are depicted in, and the arrangement of shear walls in each model is described below as Model-1 to Model-9:

Model-1: Rectangular building without any shear wall.

Model-2: Buildings with shear walls located at all four corners-1.

Model-3: Buildings with shear walls located at all four corners-2.

Model-4: Buildings with shear walls located at only two opposite corners.

Model-5: Buildings with shear walls located at all four edges.

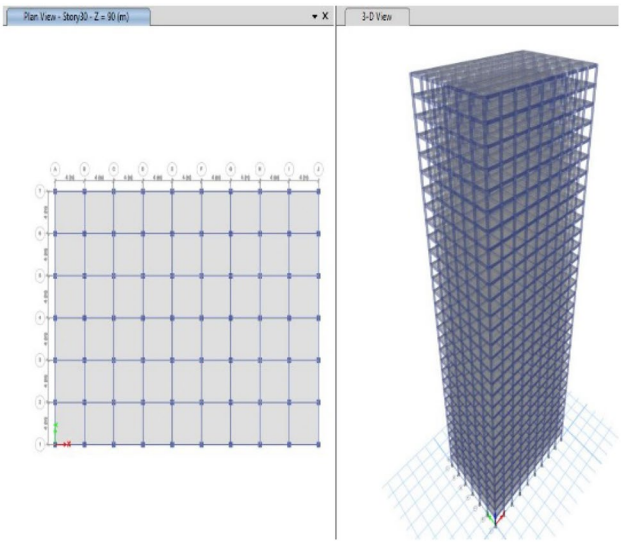

Fig. 1 Model-1: Building without any shear wall

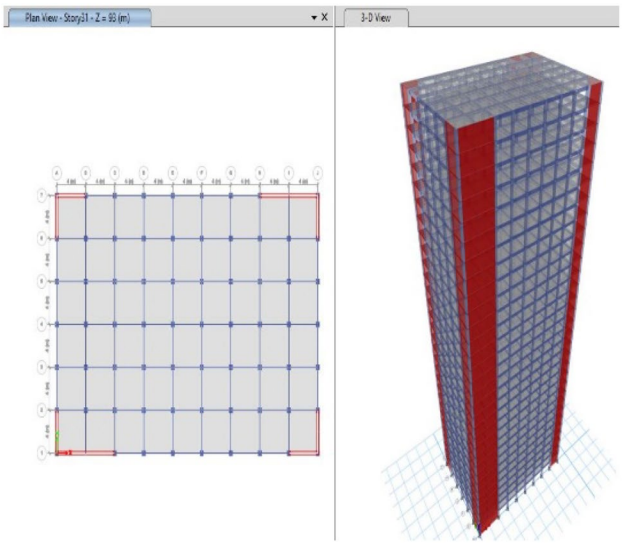

Fig. 2 Model-2: Buildings with shear walls located at all four corners-1

Model-6: Buildings with shear wall located at the centre as core.

Model-7: Buildings with shear walls located at two opposite edges and centre.

Model-8: Buildings with shear wall located at the centre in E-shape.

Model-9: Building with a shear wall located at the centre in I-shape.

The floor plan and 3D view of the above models will be shown in Figs. 1, 2, 3, 4, 5, 6, 7, 8 and 9, respectively. The fixed supports have been provided at the base of each building making it a vertical cantilever.

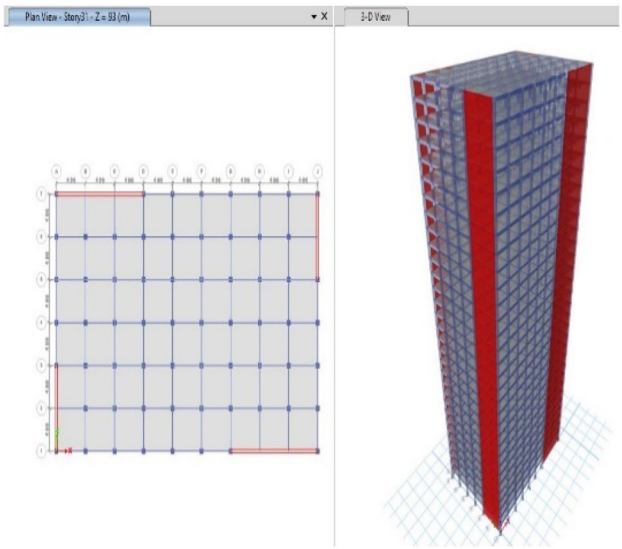

Fig. 3 Model-3: Buildings with shear wall located at all four corners-2

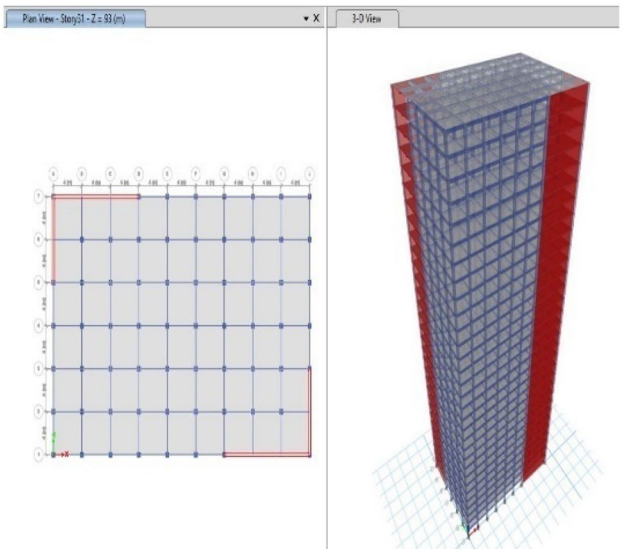

Fig. 4 Model-4: Buildings with shear walls located at only two opposite corners

Dimensional configurations

The 3D grid has been inserted with 10 and 7 gridlines parallel to Y- and X-direction, respectively, and 31 floors. Beams and columns are specified as 1D frame elements, whilst slabs and shear walls are defined as 2D shell components.

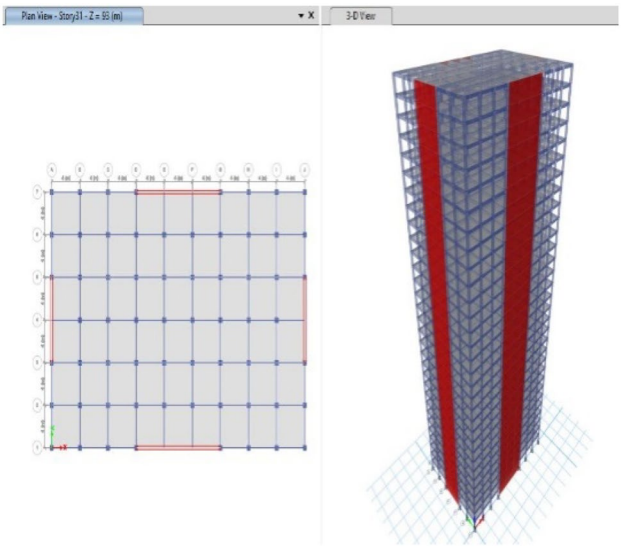

Fig. 5 Model-5: Buildings with shear wall located at all four edges

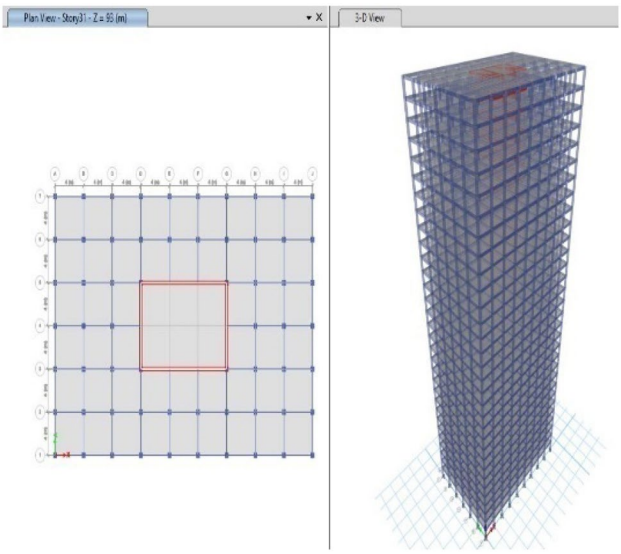

Fig. 6 Model-6: Buildings with shear wall located at the centre as core

Table 1 displays dimension data for each element's size. The entire floor plan length of the shear wall is the same in all models; only the placement differs.

Material properties

The various properties of concrete and steel are loaded into the software for analysis. Concrete is taken to be homogeneous, isotropic and elastic. The other properties of both materials used in modelling are given in Table 2.

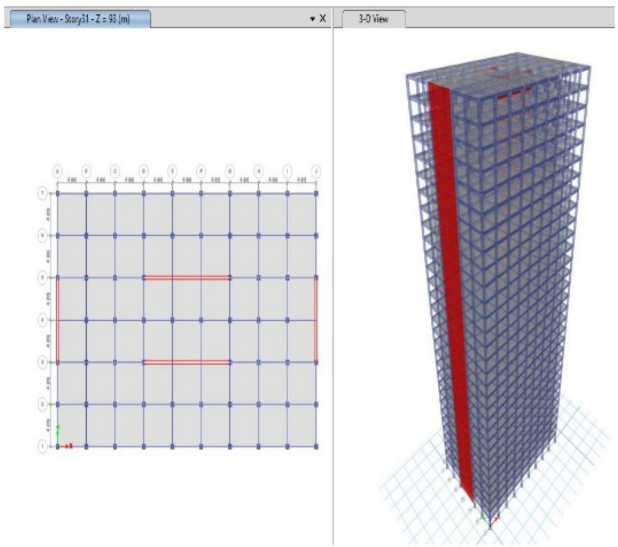

Fig. 7 Model-7: Buildings with shear wall located at two opposite edges and centre

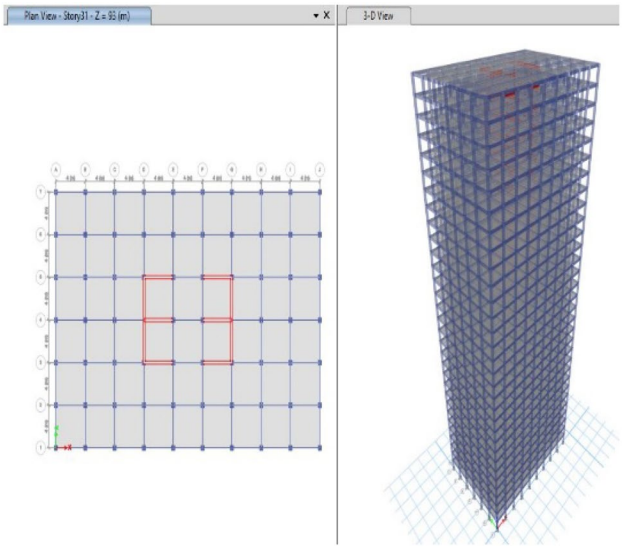

Fig. 8 Model-8: Buildings with shear wall located at the centre in E-shape

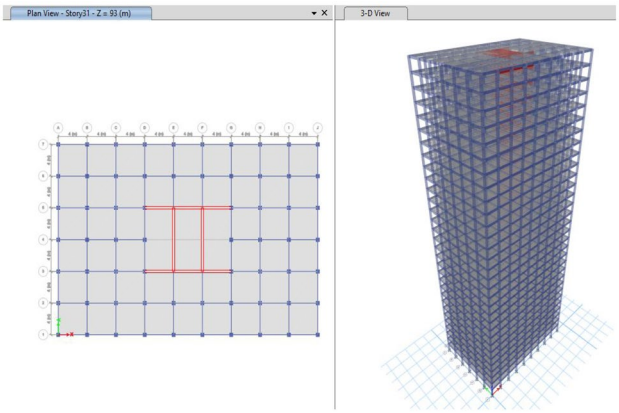

Fig. 9 Model-9: Building with shear wall located at the centre in I-shape

Table 1 Dimension configurations

No. of bays along the X-direction	9
No. of bays along the Y-direction	6
Length of each bay (m)	4
Height of each floor (m)	3
Total height of buildings (m)	93
Size of the beam (mm × mm)	300×450
Size of column (mm × mm)	500×500
The thickness of the slab (mm)	150
The thickness of the shear wall (mm)	300

Table 2 Material properties

Material	Concrete	Steel
Grade	M30	Fe415
Specific weight (γ) kN/m^3	25	76.97
Density (ρ) kg/m^3	2549.29	7849.05
Modulus of elasticity(E) MPa	2.74×10^4	2×10^5
Poisson's ratio (μ)	0.2	–
Coefficient of thermal expansion (1/°C)	10×10^{-6}	12×10^{-6}
Shear modulus (G) MPa	1.14×10^4	–

Numerical evaluation of natural frequency and mode shape of the system

Before diving into a dynamic analysis, a modal analysis must be conducted. Modal analysis is capable of capturing the dynamic features of the vibrating system, such as its mode shapes and natural frequency.

Equation (1), damping and force matrix terms are neglected for un-damped free vibration systems. The fundamental formula of vibration for a free-vibrating system with no damping may be expressed as (1):

$$[M]\left[\ddot{\delta}\right] + [K][\delta] = 0 \tag{1}$$

where $[\delta]$, $\left[\ddot{\delta}\right]\left[\dot{\delta}\right]$ are the global displacement, acceleration and velocity vector matrix values, $[M]$, $[K]$ and [C] are the global mass, stiffness and damping matrix.

Under the assumption of harmonic motion in the natural mode of vibration, the solution of displacement may be expressed as (2)

$$[\delta] = [X]\sin(\omega t + \varphi) \tag{2}$$

where $[X]is$ the vector of the nodal amplitude of vibration, ω is the circular natural frequency of vibration [rad/sec] and φ is the phase angle.

Substitution of (2) in (1) leads to the generalised eigenvalue problem.

$$\left[[K] - \omega^2[M]\right][X] = 0 \tag{3}$$

Solving (3) with a basic eigen solver yields the natural frequencies and mode shapes of any structural system.

To get the building dynamic characteristics, Eq. (3) is solved using a common eigen solver.

The theoretical natural frequency as mentioned in Chopra, (2012), can be written as:

$$f_n = n^2\pi^2\sqrt{\frac{EI}{mL^4}}\ n = 1, 2, 3, \tag{4}$$

where f_n is the frequency of each order, EI is the flexural stiffness of the cross-section, m is mass per unit length and L is the length of the beam.

$$\varnothing_n(x) = C_1 \sin\frac{n\pi x}{L} \tag{5}$$

where $\varnothing_n$ denotes the corresponding mode shape.

Loading details

The dead load, live load and seismic loads are used to conduct the structure analysis. The dead loads are calculated using the density of the material and provided dimensions of various elements in the software automatically. The floor finish load on each floor and the roof is assumed to be 1 kN/m^2. The live load on the floors and roof is calculated using IS 875, Part-2. (1987), which is 2 kN/m^2 and 1.5 kN/m^2, respectively. As shown in Table 3, the seismic analysis is carried out using the response spectrum method as per IS, 1893, Part-1. (2016). Figure 10 depicts the response spectrum curve of the period (T) vs. acceleration (a).

Table 3 Seismic data

Zone factor (Z)	0.16
Importance factor (I)	1
Response reduction factor (R)	5
Site type	2 (Medium soil)
Damping ratio (ζ)	5%

Results and discussion

Model analysis

The free vibration analysis was performed in ETABS software using the eigenvalue approach, and the results of parameters such as natural time period and corresponding frequency, modal directional factor, and mass participation factor were extracted. As a result, the following section will go over the outcomes of these parameters.

Modal directional factor

The study should be performed in such a way that the maximum dead weight of the structure participates in the vibration. As a result, 12 modes are extracted until 95 percent of the mass participates. Buildings vibrate in different directions for each mode, with three types of vibration: translation vibration in the X-direction (UX), translation vibration in the Y-direction (UY) and torsional vibration (RZ). The

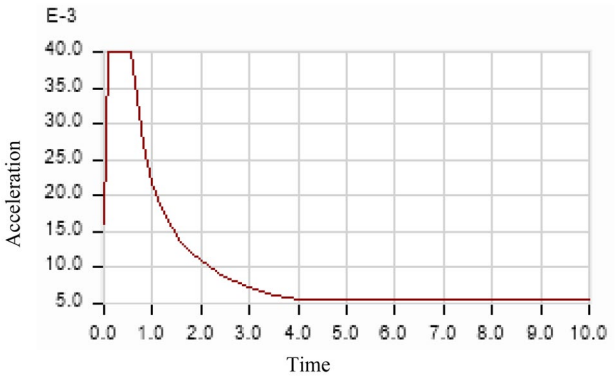

Fig. 10 Response spectrum curve

Table 4 The modal directional factor for Model-2

Case	Mode	UX	UY	RZ
Modal	1	0.009	0.991	0
Modal	2	0.991	0.009	0
Modal	3	0	0	1
Modal	4	0.017	0.983	0
Modal	5	0.983	0.017	0
Modal	6	0	0	1
Modal	7	0.019	0.981	0
Modal	8	0.98	0.02	0
Modal	9	0.016	0.984	0
Modal	10	0	0	1
Modal	11	0.954	0.046	0
Modal	12	0.042	0.958	0

Table 5 The vibration of all the models in each mode

Mode	X-direction translation	Y-direction translation	Torsional
1	Model-1, 8	Model-2, 3, 4, 5, 6, 7, 9	–
2	Model-2, 3, 4, 5, 6, 7	Model-1, 8	Model-9
3	Model-9	–	Model-1, 2, 3, 4, 5, 6, 7, 8
4	Model-1, 8	Model-2, 3, 4, 5, 6, 7	Model-9
5	Model-2, 3, 4, 5, 6	Model-1, 9	Model-7, 8
6	Model-7, 9	Model-8	Model-1, 2, 3, 4, 5, 6
7	Model-1	Model-2, 3, 4, 5, 6, 7	Model-8, 9
8	Model-2, 3, 4, 5, 8	Model-1, 9	Model-6, 7
9	Model-6, 7	Model-2, 4, 5, 8	Model-1, 3, 9
10	Model-1, 9	Model-3, 7	Model-2, 4, 5, 6, 8
11	Model-2, 3, 5, 8	Model-1, 4, 6	Model-7, 9
12	Model-4, 7	Model-2, 3, 5, 9	Model-1, 6, 8

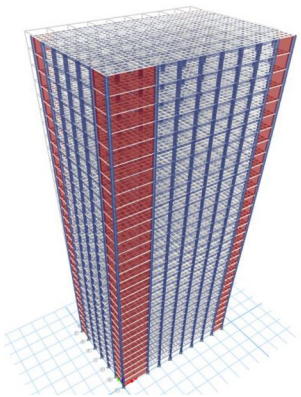

Fig. 11 Mode-1 (first mode of Y-dir. Trans.) f = 0.37 Hz

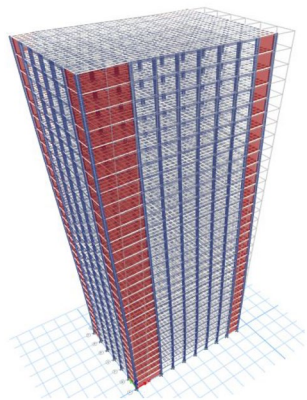

Fig. 12 Mode-2 (first mode of X-dir. Trans.) f = 0.45 Hz

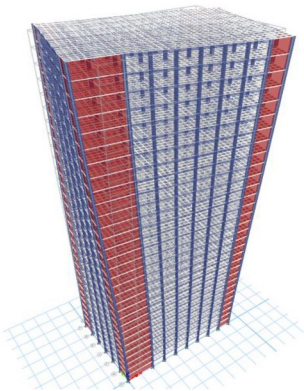

Fig. 13 Mode-3 (first mode of Torsion) f = 0.54 Hz

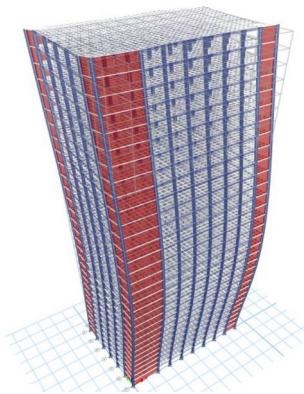

Fig. 14 Mode-4 (second mode of Y-dir. Trans.) f = 1.28 Hz

modal directional factor represents the fraction of vibration that occurs in a particular direction for a particular mode. Table 4 displays the directional factor in each direction for all modes in Model-2.

The vibration of all models can be determined using such modal directional factor tables, which are summarised in Table 5. The principal vibrational direction has been represented in this table, whilst a minor fraction of vibration in the other direction has been ignored (ex. the primary

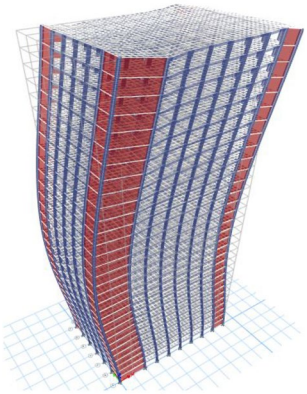

Fig. 15 Mode-5 (second mode of X-dir. Trans.) f = 1.68 Hz

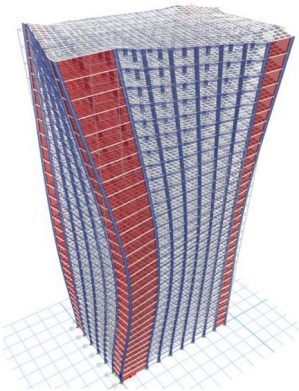

Fig. 16 Mode-6 (second mode of Torsion) f = 2.12 Hz

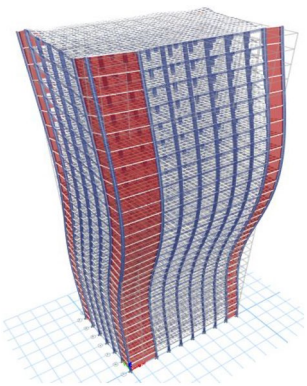

Fig. 17 Mode-7 (third mode of Y-dir. Trans.) f = 2.60 Hz

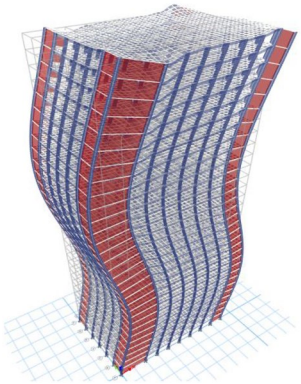

Fig. 18 Mode-8 (third mode of X-dir. Trans.) f = 3.67 Hz

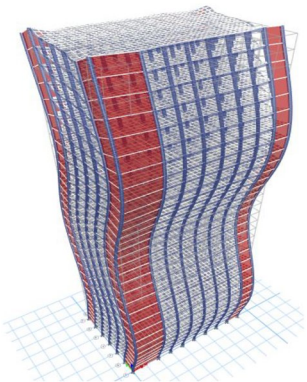

Fig. 19 Mode-9 (fourth mode of Y-dir. Trans.) f = 4.31 Hz

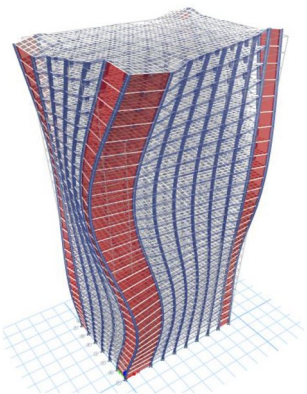

Fig. 20 Mode-10 (third mode of torsion) f = 4.85 Hz

vibrational direction UY is considered from the first mode of Model-2, as seen from, whereas UX is ignored).

Figures 11, 12, 13, 14, 15, 16, 17, 18, 19, 20, 21 and 22 illustrate mode shape diagrams of such vibrations of only

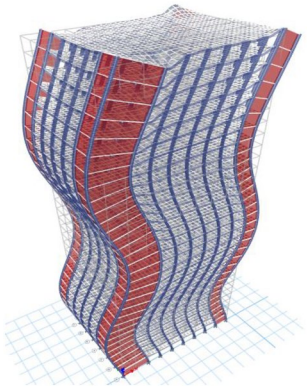

Fig.21 Mode-11 (fourth mode of X-dir. Trans.) f = 6.20 Hz

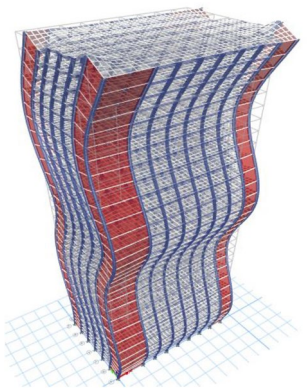

Fig. 22 Mode-12 (fifth mode of Y-dir. Trans.) f = 6.37 Hz

one structure (Model-2) for reference to provide a clear visualisation of vibrations.

Mass participation factor

In the first mode, mass participation ranges between 65 and 70% for each model in their principal vibrational direction. Up to the sixth mode, there was approximately 85% mass participation in both UX and UY directions for all models. As a result, these are the most important modes of vibration. In the twelfth mode, almost 95% of the mass participated in all three vibrational directions for each model. Tables 6 and 7 show the cumulative mass involvement for the first sixth and twelfth modes for all models in the UX and UY directions.

Time period (T) comparison

The results of the time period and frequencies for different modes in Model-2 has been shown in Table 8. Time periods of various models can be compared using similar tables retrieved from ETABS, as shown in Fig. 23. The model with no shear wall exhibits the longest time period for each mode. The inclusion of a shear wall increases the stiffness of the structure, resulting in a smaller time period.

The time period has decreased by approximately 16, 20, 25, 22, 35, 20, 26 and 33% for Model-2, 3, 4, 5, 6, 7, 8 and 9, respectively. Model-6 indicates a significant decline of 60–67% for 3 to 12 modes, with a maximum decrease of 66.93% for the 12th mode. Model-4 has the largest decrement of all models, around 70% in the 12th mode.

The ETABS software was used to calculate the results of parameters such as maximum storey displacements, maximum storey drifts and maximum storey shear. Comparison charts have been created for each parameter to give an idea of how the height of the building has affected the variation in parameters for each model. Model-2 to Model-9 top displacements were compared to Model-1 top displacements.

Figure 24 shows the results of the displacement of models subjected to seismic loading calculated with the response spectrum method. When the models are subjected to earthquake loads in the X-direction in various configurations, the E-centre wall building and core wall buildings exhibit maximum and minimum displacement at the top. In comparison to a rectangle building with no shear wall, the displacement of various buildings is reduced by 1.64 times for the E-centre wall, 2.47 times for the edge wall, 2.89 times for the opposite corner wall, 2.48 times for the I-centre wall, 2.57 times for the edge and centre wall, 1.97 times for the corner wall, 2.28 times for the corner wall 2 and 3.23 times for the core wall.

Table 6 Mass participation percentage

Modes	Model-1		Model-2		Model-3		Model-4		Model-5	
	UX	UY	UX	UY	UX	UY	UX	UY	UX	UY
1	0	78.14	0.66	71.79	0.02	71.09	5.38	65.23	0	71.26
2	79.28	78.14	69.82	72.36	68.72	71.11	68.06	69.8	69.32	71.26
3	79.28	78.14	69.82	72.36	68.72	71.11	68.06	69.8	69.32	71.26
4	79.28	89.77	69.99	84.63	68.72	84.49	69.47	82.05	69.32	84.68
5	89.92	89.77	84.18	84.92	84.12	84.49	84.8	84.69	84.31	84.68
6	89.92	89.77	84.18	84.92	84.12	84.49	84.8	84.69	84.31	84.68
12	95.14	95.1	93.35	94.76	93.67	95.04	94.53	95.33	93.7	95.07

Table 7 Mass participation percentage

Modes	Model-6		Model-7		Model-8		Model-9	
	UX	UY	UX	UY	UX	UY	UX	UY
1	0	67.94	0	70.61	72.55	0	0	68.91
2	67.63	67.94	69.62	70.61	72.55	68.34	0	68.91
3	67.63	67.94	69.62	70.61	72.55	68.34	68.9	68.91
4	67.63	85.07	69.62	84.66	84.88	68.34	68.9	68.91
5	85.21	85.07	69.62	84.66	84.88	68.34	68.9	85.83
6	85.21	85.07	84.49	84.66	84.88	85.07	84.55	85.83
12	91.6	94.44	93.75	93.15	92.77	91.17	90.64	94.26

Table 8 Time period and corresponding frequencies

Case	Mode	Period (T) Sec	Frequency (f) Hz	Circular Freq. (ω) Rad/sec	Eigenvalue (λ) Rad^2/sec^2
Modal	1	2.70	0.37	2.33	5.44
Modal	2	2.24	0.45	2.81	7.87
Modal	3	1.87	0.54	3.36	11.31
Modal	4	0.78	1.28	8.04	64.56
Modal	5	0.60	1.68	10.52	110.75
Modal	6	0.47	2.12	13.33	177.77
Modal	7	0.38	2.60	16.35	267.16
Modal	8	0.27	3.67	23.04	530.80
Modal	9	0.23	4.31	27.06	732.08
Modal	10	0.21	4.85	30.50	930.03
Modal	11	0.16	6.20	38.98	1519.22
Modal	12	0.16	6.37	40.01	1601.15

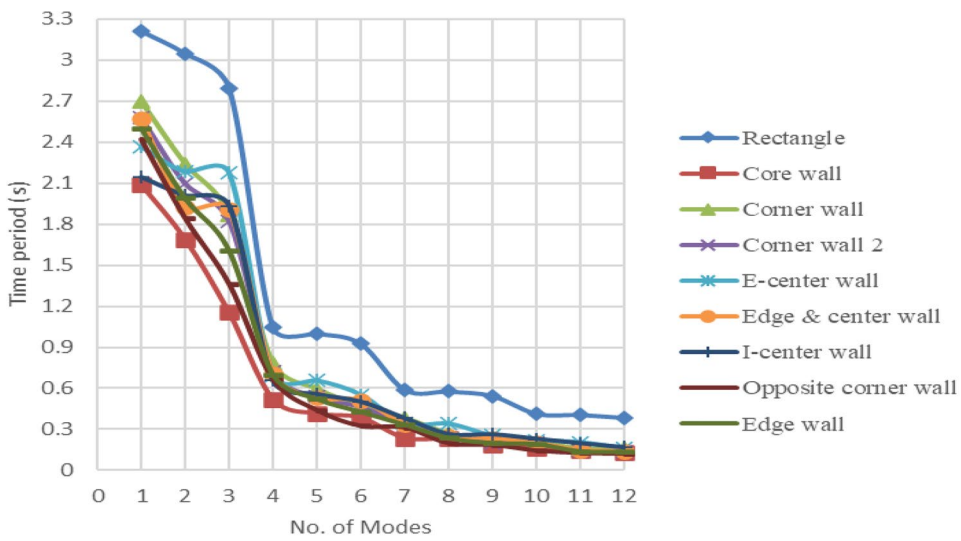

Fig. 23 Time period comparison

The introduction of shear walls also decreases drift in buildings because of an increment in stiffness (Fig. 25). There has been an increment in a drift up to a certain storey depending upon the arrangement of walls, followed by a decrement at a much slower rate for models with shear walls than Model-1. So, Model-1 has experienced less drift at the top storey. In addition, in all models with the shear wall, there is less difference between drifts of two adjacent storeys. Model-6 shows the minimum drift value compared to others. When compared to other models with shear walls, Model-8 drifts more at lower storeys.

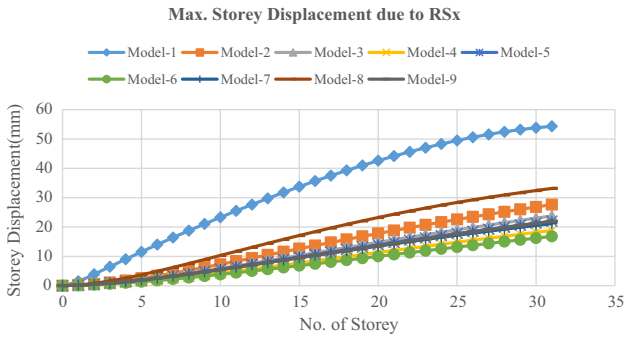

Fig. 24 Max storey displacement in X-direction

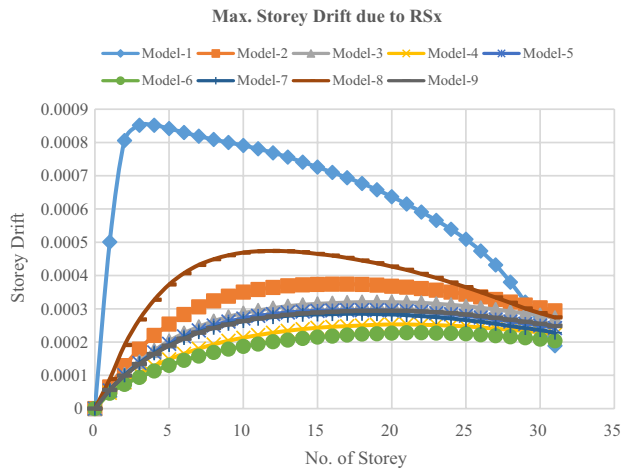

Fig. 25 Max storey drift in X-direction

Fig. 26 Storey shear in X-direction

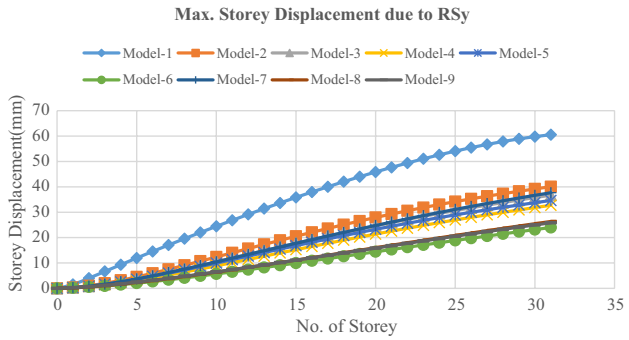

Fig. 27 Max storey displacement in Y-direction

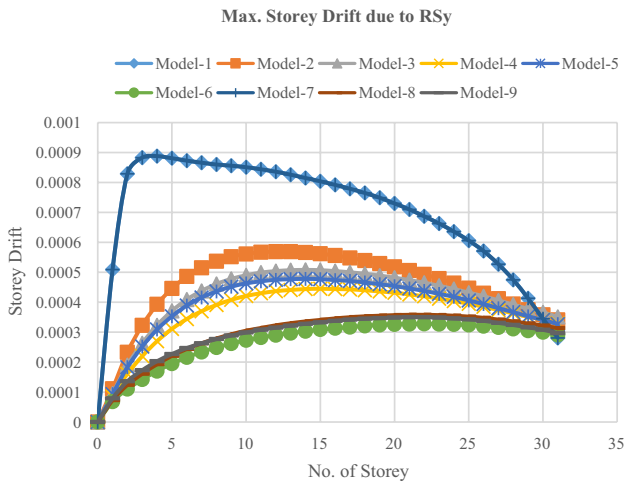

Fig. 28 Max storey drift in the Y-direction

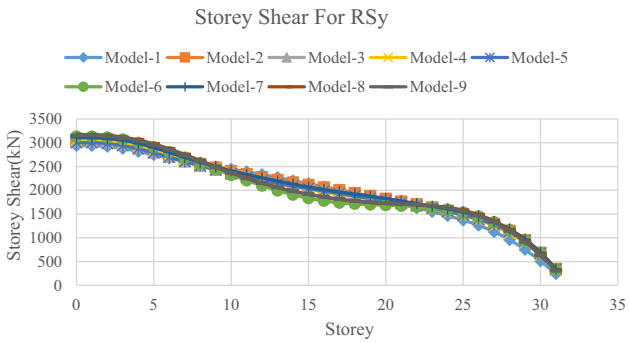

Fig. 29 Storey shear in Y-direction

With the addition of shear walls to the models, the shear force increases as shown in Fig. 26. In all buildings with shear walls, there has been a significant increase in shear forces at the top storeys and a minor increase at the base. In Model-2, 3, 4, 5, 6, 7, 8 and 9, top storey shear increases by 35.12, 33.26, 17.44, 31.04, 20.57, 31.47, 36.66 and 28.91% compared to Model-1, respectively. The values of base shear increase just by 3.20, 1.97, 1.98, 2.58, 5.83, 5.19, 8.23 and 7.50 for Model-2, 3, 4, 5, 6, 7, 8 and 9, respectively.

Figure 27 depicts the results of displacement that occur in response to seismic forces in the Y-direction. When earthquake forces are applied in the Y-direction, the minimum and maximum displacements are experienced by the core

wall and corner wall 1 (2.52 and 1.51 times less than the building without the shear wall, respectively). In comparison to a rectangle, corner wall 2 displaces 1.65 times, E-centre wall displaces 2.3 times, edge and centre wall displaces 1.61 times, I-centre wall displaces 2.34 times, opposite corner wall displaces 1.85 times and edge wall displaces 1.75 times lesser than rectangle building. Buildings have drifted in the Y-direction in the same way that they have drifted in the X-direction (Fig. 28). Here, Model-6 gets the minimum drift value amongst all models. Model-2 shows maximum drift values amongst all the models.

In comparison to Model-1, top-storey shear increases by 37.63, 39.21, 26.17, 35.30, 28.03, 37.07, 25.65 and 20.48% in Models-2, 3, 4, 5, 6, 7, 8 and 9. The values of shear at a base increase by 4.25, 3.62, 5.09, 2.98, 7.46, 6.61, 8.91 and 8.30 for Models-2, 3, 4, 5, 6, 7, 8 and 9, respectively. A comparison of storey shear for all nine models is shown in Fig. 29.

Conclusion

As important constructions are influenced by seismic vibration, high-rise buildings must be precisely built. Before completing the dynamic analysis, it is critical to undertake a free vibration study of the structure. In this work, the free vibration response of a range of high-rise buildings with and without shear walls was given. This current study has presented the responses of various models subjected to seismic loads. The following is a concise conclusion of the overall analyse.

1. As the stiffness of the model increases due to the shear wall, the natural time period decreases in all models with the shear wall.
2. In the case of a shear wall arranged just in the centre of the building, there is a considerably higher time period decrement when compared to other models, with the core form of arrangement presenting the greatest decrement in fundamental mode.
3. Models with shear walls at all four corners have the smallest time period decrement.
4. Model-6, with shear walls arranged in the form of a core at the centre of the building, has been the most efficient in resisting lateral loads in both directions.
5. It cannot be claimed from the research that shear walls at the centre location always perform better, as Model-8 has performed with poor efficiency against lateral loads in the X-direction, leading to the conclusion that not only location but the arrangement of walls also plays an important role.
6. It has been seen that buildings with walls located at the corners are more vulnerable to seismic loads compared to buildings with properly arranged walls at the centre and buildings with shear walls located at the edges.
7. Buildings with walls located at the edges and centre have outperformed, compared to buildings with walls located only at the edges.

Limitations and implications of the research

The research mainly focussed on the free vibration and earthquake dynamics of a high-rise rectangular symmetrical building structure using the finite element software ETABS. This research will be valuable for developing high-rise rectangular buildings that account for the dynamic vibrations induced by earthquake loads, as well as further investigation of the high-rise rectangular structure model's wind dynamic behaviour. The research is confined to the vibration analysis of a high-rise rectangular building system without considering uncertainty quantification (UQ). This examination might continue with a laboratory investigation utilising a built-building model to identify the free vibration (modal) and forced vibration analysis parameters and validate the theoretical model. The research may emphasise asymmetric building shapes, with the results applicable to real-world circumstances.

Acknowledgements I want to acknowledge the Civil Engineering Department of the National Institute of Technology in Hamirpur for providing computational resources for this research.

Author contributions KS, NK: Conceptualization; KS, NK: Data curation; KS: Formal analysis; KS, NK: Investigation; KS, NK: Methodology; KS: Project administration; KS: Resources; KS: Software; NK: Supervision; KS, NK: Validation; KS, NK: Visualization; KS, NK: Roles/Writing – original draft; KS, NK: Writing – review & editing

Funding Not Applicable.

Data availability The data that were used in this research was produced using simulation results. The model and inputs are accessible via email at nallasivam_iit_nit@yahoo.co.in.

Declarations

Conflict of interest No competing interests are foreseen.

Ethical approval Not applicable.

Consent to participate Not applicable

Consent for publication Not applicable

References

Abd-el-Rahim, H. H. A., & Farghaly, A. A. E. R. (2010). Role of shear walls in high rise buildings. *JES Journal of Engineering Sciences, 38*(2), 403–420. https://doi.org/10.21608/jesaun.2010.124373

Agha, W. A., & Umamaheswari, N. (2020). Analytical study of an irregularly reinforced concrete building with shear wall and dual framed-shear wall system by using equivalent static and response spectrum methods. *Materials Today: Proceedings., 43*, 2232–2241. https://doi.org/10.1016/j.matpr.2020.12.525

Akhil-Ahamad, S., & Pratap, K. V. (2020). Dynamic analysis of G+20 multi-storied building by using shear walls in various locations for different seismic zones by using Etabs. *Materials Today: Proceedings, 43*, 1043–1048. https://doi.org/10.1016/j.matpr.2020.08.014

Bhatt, C., & Bento, R. (2012). Comparison of nonlinear static methods for the seismic assessment of plan irregular frame buildings with non-seismic details. *Journal of Earthquake Engineering, 169*(1), 15–39. https://doi.org/10.1080/13632469.2011.586085

Chopra, A. (2012). *Dynamics of Structures* (4th ed.). Pearson.

Fan, H., Li, Q. S., Tuan, A. Y., & Xu, L. (2009). Seismic analysis of the world's tallest. Building. *Journal of Constructional Steel Research, 65*(5), 1206–1215. https://doi.org/10.1016/j.jcsr.2008.10.005

Ghayoumian, G., & Emami, A. R. (2020). A multi-direction pushover procedure for seismic response assessment of low-to-medium-rise modern reinforced concrete buildings with the special dual system having torsional irregularity. *Structures, 28*, 1077–1107. https://doi.org/10.1016/j.istruc.2020.09.031

IS 1893, Part-1 (2016). Criteria for Earthquake resistant design of structures, Part 1: General Provisions and Buildings. 6th Revision. Bureau of Indian Standard, New Delhi

IS 875, Part-2. (1987) Reaffirmed 2008. Code of Practice for Design Loads (Other Than Earthquake) For Buildings and Structures: Imposed Loads. 2nd Revision. Bureau of Indian Standards, New Dehli

Kaveh, A., & Bolandgerami, A. (2017). Optimal design of large scale space steel frames using cascade enhanced colliding body optimization. *Structural Multidisciplinary Optimization, 55*, 237–256.

Kaveh, A., Farahmand-Azar, B., Hadidi, A., Rezazadeh-Sorochi, F., & Talatahari, S. (2010). Performance-based seismic design of steel frames using ant colony optimization. *Journal of Constructional Steel Research, 66*(4), 66566–66574.

Kaveh, A., Kalateh-Ahani, M., & Fahimi-Farzam, M. (2014a). Life-cycle cost optimization of steel moment-frame structures: Performance-based seismic design approach. *Earthquakes and Structures, 7*(3), 271–294.

Kaveh, A., Kalateh-Ahani, M., & Fahimi-Farzam, M. (2014b). Damage-based optimization of large-scale steel structures. *Earthquakes and Structures, 7*(3), 1119–1139.

Kaveh, A., & Talatahari, S. (2010). An improved ant colony optimization for design of steel frames. *Engineering Structures, 32*(3), 32864–32873.

Kaveh, A., & Talatahari, S. (2012). Charged system search for optimal design of planar frame structures. *Applied Soft Computing, 12*(1), 382–393.

Kaveh, A., & Zakian, P. (2013). Optimal design of steel frames under seismic loading using two meta-heuristic algorithms. *Journal of Constructional Steel Research, 82*, 111–130.

Kaveh, A., & Zakian, P. (2014). Seismic design optimisation of RC Moment frames and dual shear wall-frame structures via CSS algorithm. *Asian Journal of Civil Engineering, 15*, 435–465.

Murty, C. V. R. (2005). Learning earthquake design and construction. *Resonance, 10*(11), 85–88. https://doi.org/10.1007/bf02837648

Smith, B. S., & Coull, A. (1991). *Tall building structures: Analysis and design*. John Wiley & Sons. Inc.

Titiksh, A., & Bhatt, G. (2017). Optimum positioning of shear walls for minimizing the effects of lateral forces in multistorey-buildings. *Archives of Civil Engineering, 63*(1), 151–162. https://doi.org/10.1515/ace-2017-0010

Tuppad, S., & Fernandes, R. J. (2015). Optimum location of shear wall in a multi-storey building subjected to seismic behavior using genetic algorithm. *International Research Journal of Engineering and Technology, 2*(4), 236–240.

Udaya, B. K., Manish, K. G., & Senthil P. M. (2018). Dynamic analysis of multi-storey building. *Journal of Industrial Pollution Control*, 1–12.

Wang, Q., Wang, L., & Liu, Q. (2001). Effect of shear wall height on earthquake response. *Engineering Structure, 23*(4), 376–384. https://doi.org/10.1016/S0141-0296(00)00044-4

Zakian, P., & Kaveh, A. (2023). Seismic design optimization of engineering structures: A comprehensive review. *Acta Mechanica, 234*, 1305–1330.

Publisher's Note Springer Nature remains neutral with regard to jurisdictional claims in published maps and institutional affiliations.

Springer Nature or its licensor (e.g. a society or other partner) holds exclusive rights to this article under a publishing agreement with the author(s) or other rightsholder(s); author self-archiving of the accepted manuscript version of this article is solely governed by the terms of such publishing agreement and applicable law.